Taylor & Francis
Taylor & Francis Group

Check for updates

Drug repositioning to propose alternative modulators for glucocorticoid receptor through structure-based virtual screening

Reyhan Metin[a] and Ebru Demet Akten[b]

[a]Graduate Program of Computational Biology and Bioinformatics, Graduate School of Science and Engineering, Kadir Has University, Istanbul, Turkey; [b]Department of Bioinformatics and Genetics, Faculty of Engineering and Natural Sciences, Kadir Has University, Istanbul, Turkey

Communicated by Ramaswamy H. Sarma

ABSTRACT

Drug repositioning has recently become one of the widely used drug design approaches in proposing alternative compounds with potentially fewer side effects. In this study, structure-based pharmacophore modelling and docking was used to screen existing drug molecules to bring forward potential modulators for ligand-binding domain of human glucocorticoid receptor (hGR). There exist several drug molecules targeting hGR, yet their apparent side effects still persist. Our goal was to disclose new compounds via screening existing drug compounds to bring forward fast and explicit solutions. The so-called *shared* pharmacophore model was created using the most persistent pharmacophore features shared by several crystal structures of the receptor. The *shared* model was first used to screen a small database of 75 agonists and 300 antagonists/decoys, and exhibited a successful outcome in its ability to distinguish agonists from antagonists/decoys. Then, it was used to screen a database of over 5000 molecules composed of FDA-approved, worldwide used and investigational drug compounds. A total of 110 compounds satisfying the pharmacophore requirements were subjected to different docking experiments for further assessment of their binding ability. In the final hit list of 54 compounds which fulfilled all scoring criteria, 19 of them were nonsteroidal and when further investigated, each presented a unique scaffold with little structural resemblance to any known nonsteroidal GR modulators. Independent 100 ns long MD simulations conducted on three selected drug candidates in complex with hGR displayed stable conformations incorporating several hydrogen bonds common to all three compounds and the reference molecule dexamethasone.

Introduction

As a steroid hormone activated transcription factor, glucocorticoid receptor (GR) belongs to the superfamily of ligand-regulated nuclear receptors (NRs) comprising the estrogen receptor (ER), progesterone receptor (PR), androgen receptor (AR), mineralocorticoid receptor (MR), peroxisome proliferation receptor, vitamin D receptor and the thyroid hormone receptor. It has an important role for inflammation response, and is involved in the control of cell growth, apoptosis, differentiation and metabolism (Bereshchenko et al., 2018; Kadmiel & Cidlowski, 2013). It is a ubiquitously expressed intracellular protein that regulates gene transcription. Following the first X-ray crystal structure resolved by Bledsoe *et al.* in 2002 (Bledsoe et al., 2002), the GR ligand binding domain has become the target of all rational drug-design studies conducted in the last twenty years towards finding selective agonists that possess the desired anti-inflammatory and immunosuppressive properties with fewer side effects.

Expressed by NR3C1 gene which is located on chromosome 5 (5q31), GRs have a modular structure which consists of several domains listed in sequential order; N-terminal transactivation domain (NTD, 1 to 421 residues), DNA binding domain (DBD, 422 to 486 residues), a hinge region (486 to 528 residues), ligand binding domain (LBD, 528 to 777 residues) and a C-terminal domain (Oakley & Cidlowski, 2011). The receptor consists mainly of alpha helices and a few beta sheets that fold into a three-layered alpha-helical domain which creates a fully occluded ligand-binding pocket surrounded by four helices. As a result of a ligand binding which triggers a conformational rearrangement in LBD, the receptor is released from the heteromeric complex which consists of several chaperone proteins including heat-shock protein HSP90, and enters the nucleus where it regulates gene expression directly or indirectly, through interacting with site-specific DNA sequences and several other coregulatory proteins and transcription factors.

Glocucorticoids (GCs) are the natural steroid ligands of GRs. Since 1950s, they have been widely used in the treatment of inflammatory and autoimmune diseases. However, their desired anti-inflammatory and immunosuppressive effects were often accompanied by adverse side effects such

as diabetes mellitus, glaucoma, hypertension, Cushing's syndrome, osteoporosis and many others (Schake et al., 2002). GCs in complex with GRs regulate gene transcription by both transactivation and transrepression mechanisms. Many detrimental steroidal side effects are caused by transactivation whereas transrepression is considered as the key mechanism for the antiinflamatory activity. Over the years, there have been several attempts to identify ligands which preferentially induce transrepression with little or no transactivating mechanism. One such study by Schacke et al. more than a decade ago introduced a nonsteroidal selective GR agonist (SEGRA) called ZK216348 which showed a markedly superior side effect profile in addition to an improved therapeutic index comparable to classical GCs (Schäcke et al., 2004). However, ZK216348 displayed a poor selectivity, binding to progesterone receptor (PR), androgen receptor (AR) and mineralocorticoid receptor (MR) in addition to GR. In later years, the same research group redesigned ZK216348 to increase the selectivity towards GR by replacing the methylbenzoxazine with a quinoline moiety and came up with a prototype with reduced activity in a transactivation assay (Jaroch et al., 2010). In fact, the quinoline core was presented as a novel scaffold in an early study by Coghlan et al. which reported the first nonsteroidal GR-selective ligands with functional profiles similar to those of natural GCs (Coghlan et al., 2001). In the last two decades, several other nonsteroidal ligands such as ZK245186, CpdA, LGD5552, Org214007-0, Mapracorat, Dagrocorat and indazole ethers were presented as promising GR modulators which strongly binds GR and represses inflammatory gene expression both *in vitro* and *in vivo* studies (Baiula & Spampinato, 2014; De Bosscher et al., 2005; Hemmerling et al., 2017; López et al., 2008; Ripp et al., 2018; Schäcke et al., 2009; van Lierop et al., 2012). They all displayed a lower side effect compared to classical GCs.

Despite the shift towards nonsteroidal ligands due to their dissociative profile in transactivation versus transrepression, a successful attempt made by Uings et al. identified a novel steroidal GR ligand GW870086 which preserved its strong antiinflammatory effects while activating only a subset of genes that are normally activated by classical GCs (Uings et al., 2013). Thus, it was represented as a new topical steroid with a different safety profile to existing therapies. In addition, two triterpenoids, protopanaxadiol and protopanaxatriol, which share structural similarities with GCs were recently identified as potent and selective GR modulators which induced transrepressional activities with no or limited transactivation (Karra et al., 2019).

Despite several published X-ray crystal structures of GR complexed with either agonists or antagonists (Berger et al., 2017; Biggadike et al., 2008; 2009; Carson et al., 2014; Edman et al., 2014; 2015; He et al., 2014; Hemmerling et al., 2017; Madauss et al., 2008; Ripa et al., 2018; Suino-Powell et al., 2008) there is a limited amount of virtual screening studies for the discovery of GR agonists. A decade ago, an application of ligand-based virtual screening was performed for the identification of novel nonsteroidal GR modulators where a total of 264,000 commercially available compounds was screened against a pharmacophore model (Onnis et al.,

2010). More recently, Potatimis et al. used a structured-based virtual screening protocol using a pharmacophore model derived from a pyrrolidinone amide analogue (Potamitis et al., 2019). In this study, we present another structure-based screening protocol which used both pharmacophore and docking evaluations using a database which incorporated FDA-approved and World-approved drugs in addition to investigational compounds. Drug repositioning or "repurposing" of existing drug molecules has become a promising approach for identifying effective compounds in the last decade (Ashburn & Thor, 2004). The discovery of a new drug embraces many challenges which are encountered in different stages of its timeline, such as *in vitro* and *in vivo* screening, toxicology tests, clinical development, and many more, each requiring several years and a substantial amount of budget. Several success stories exist in drug repositioning and thus became a well-established approach in recent years. This work is the first attempt that combines pharmacophore modelling and several docking techniques for identifying potential GR agonist candidates among the existing drug compounds.

Our pharmacophore model was generated using three X-ray crystal structures of LBD domain of hGR complexed with deacylcortivazol, dexamethasone and dibC (desisobutyrylciclesonide) in the expanded binding pocket. After an extensive elimination of compounds in the database, the remaining hit molecules were subjected to a series of docking and scoring protocols. Final hit list comprised 35 steroidal compounds which all displayed GR agonist activity, and 19 nonsteroidal compounds with unique structures which presented no marked similarity with any experimentally reported nonsteroidal GR modulators.

Methods

System preparation

A total of seventeen X-ray crystal structures of hGR complexed with various agonists were extracted from PDB databank: 3bqd, 3cld, 3e7c, 3k22, 3k23, 3csj, 4lsj, 4p6w, 4p6x, 4udd, 4udc, 5g3j, 5g5w, 5nft, 6el6, 6el7 and 6el9 (Berger et al., 2017; Biggadike et al., 2008; 2009; Carson et al., 2014; Edman et al., 2014; 2015; He et al., 2014; Hemmerling et al., 2017; Madauss et al., 2008; Ripa et al., 2018; Suino-Powell et al., 2008). After removal of all external and internal water molecules, apo forms were structurally aligned taking one structure as reference, using VMD tool (Humphrey et al., 1996). As illustrated in Figure 1a, the three-layered helical motif was observed to be strongly conserved. Moreover, RMSD values among all possible receptor pairs varied between 0.47 and 2.26 Å. Agonist molecules in seventeen complexes were categorized into two groups, steroidal and nonsteroidal. Accordingly, six steroidal and eleven nonsteroidal compounds were illustrated in Figure 1b with their chemical names and their corresponding id numbers in PDB databank.
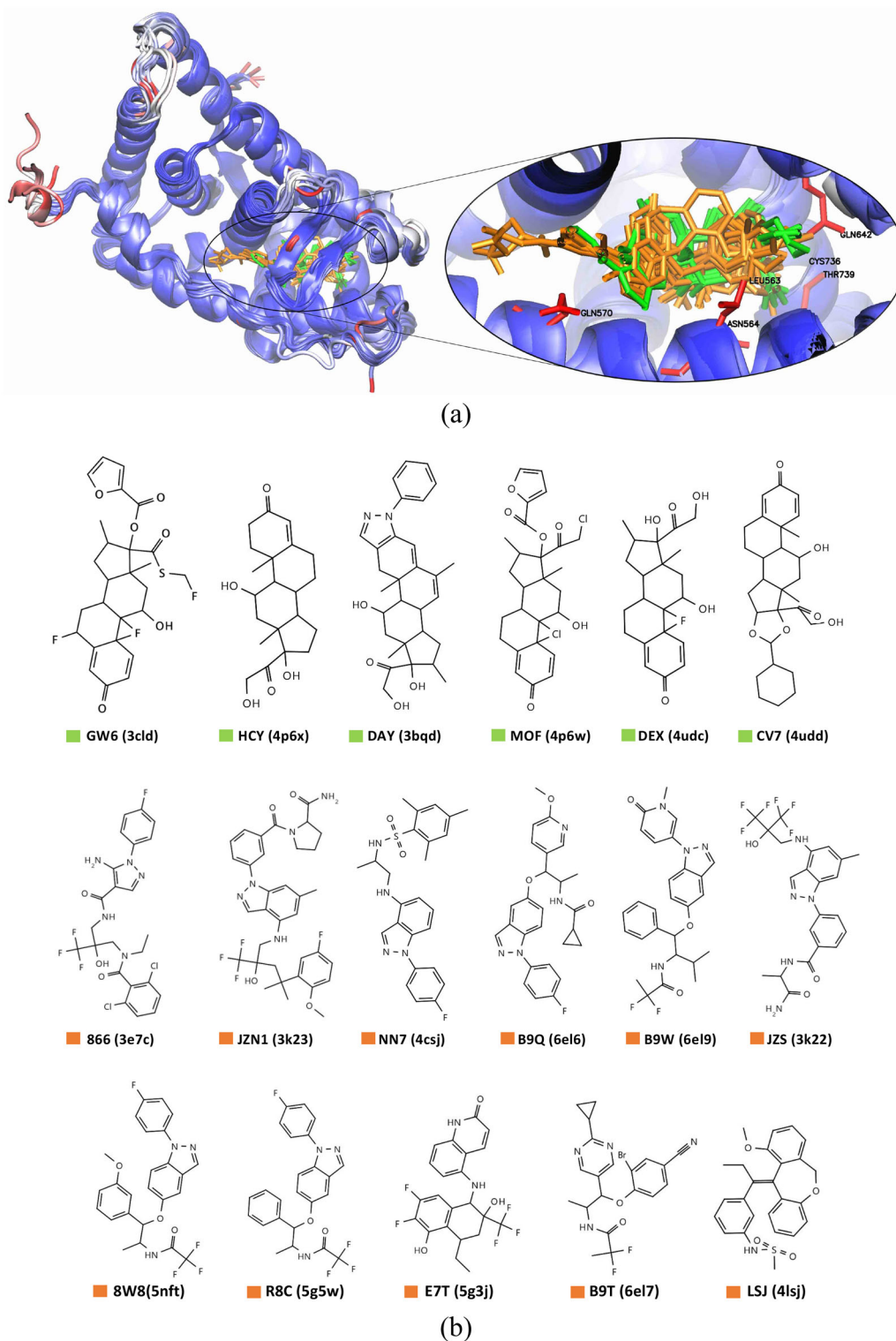
(a)

(b)

Figure 1. a) Structural alignment of seventeen GR-agonist complexes. PDB ids: 3bqd, 3cld, 3e7c, 3k22, 3k23, 3csj, 4lsj, 4p6w, 4p6x, 4udd,4udc, 5g3j, 5g5w, 5nft, 6el6, 6el7, 6el9. Sequence similarity indicated with red-white-blue color gradient where blue indicates the highest similarity and red the lowest similarity, b) 2 D representation of steroidal (with green box) and nonsteroidal GR (with orange box) agonists found in each complex structure.

Pharmacophore screening via LigandScout

A structure-based pharmacophore model was created for each seventeen complexes using the widely used LigandScout software tool (Wolber & Langer, 2005). Based on their similarities, seventeen pharmacophore models were clustered into groups of either two, three or four. Then, a so-

called "*shared*" pharmacophore model that solely consists of the common pharmacophore features was generated for each group separately. In all *shared* models, excluded volumes representing the space which was sterically occupied by the receptor were simply discarded to prevent any bias in the results, as the receptor did not occupy a fixed space around the ligand. Furthermore, 75 agonists and 300 decoys
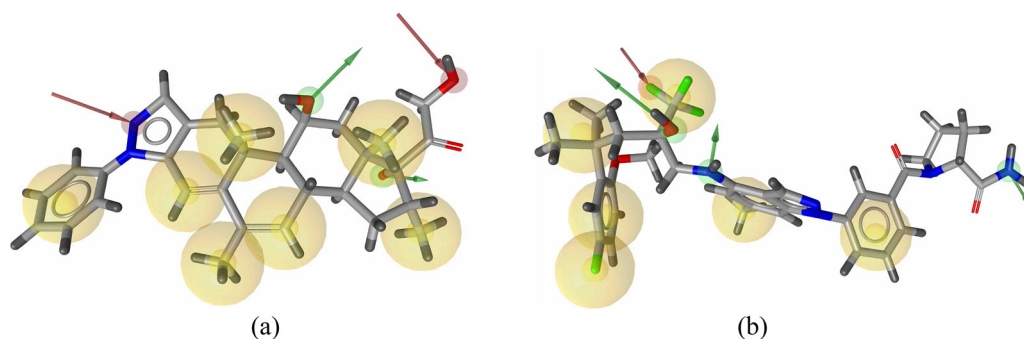
Figure 2. Structure-based pharmacophore model of (a) steroidal deacylcortivasol in 3BQD complex and (b) nonsteroidal 3S-2-pyrrolidinone amide in 3k23 complex (yellow and green/red spheres indicating atom groups involved in hydrophobic interactions and hydrogen bonding with the receptor, respectively. Green arrow emanates from hydrogen bond donor, red arrow pointing towards hydrogen bond acceptor).

Table 1. Pharmacophoric features of seventeen protein-ligand complexes along with ligand types, IDs and names.

Type	Ligand id / PDB id	Ligand Name	H-bond Donor (HBD)	H-Bond Acceptor (HBA)	Hydrophobic (HPB)
Steroidal	GW6 / 3cld (Biggadike et al., 2008)	fluticasone furoate	1	1	7
	DAY / 3bqd (Suino-Powell et al., 2008)	deacylcortivazol	2	2	7
	HCY / 4p6x (He et al., 2014)	hydrocortisone	1	3	2
	MOF / 4p6w (He et al., 2014)	mometasone furoate	1	1	5
	CV7 / 4udd (Edman et al., 2015)	desisobuytyrylciclesonide	2	4	2
	DEX / 4udc (Edman et al., 2015)	dexamethasone	3	3	4
Nonsteroidal	866 / 3e7c (Madauss et al., 2008)	aminopyrazole2,6-dichloro-N-ethylbenzamide	3	4	7
	JZS / 3k22 (Biggadike et al., 2009)	D-alaninamide derivative	3	1	5
	JZN / 3k23 (Biggadike et al., 2009)	3S-2-pyrrolidinone amide	3	1	6
	LSJ / 4lsj (Carson et al., 2014)	dibenzoxapine sulfonamide	1	2	4
	NN7 / 4csj (Edman et al., 2014)	benzene sulfonamide	2	1	7
	E7T / 5g3j (Berger et al., 2017)	compound 15 (quinoline analog)	3	1	6
	R8C / 5g5w (Hemmerling et al., 2017)	compound 1a (indazole based)	1	3	6
	8W8 / 5nft (Hemmerling et al., 2017)	AZD5423 (indazole based)	1	3	6
	B9Q / 6el6 (Ripa et al., 2018)	AZD2906 (indazole based)	1	2	6
	B9T / 6el7 (Ripa et al., 2018)	compound 31 (indazole based)	1	3	5
	B9W / 6el9 (Ripa et al., 2018)	AZD9567 (indazole based)	1	2	4

(antagonists/unknown) extracted from ZINC (Sterling & Irwin, 2015), PubChem (Kim et al., 2019) and DUD-E decoy (Mysinger et al., 2012) databases were used to construct a small database which was then screened against each of the shared models in order to test the discriminatory power. The maximum number of pharmacophore features that can be omitted during screening was set to 1, *i.e.* a hit molecule was allowed to skip one feature at most. The hit compound was further evaluated using the software tool's in-house scoring function (Wolber & Langer, 2005). A receiver operation characteristic (ROC) curve was obtained to demonstrate the model's ability to distinguish agonists from antagonists. The pharmacophore model which had the highest curve above the diagonal and also the highest AUC (area under the ROC curve) value was selected to be used for screening the large database. The large database comprised drug molecules which were either approved by major jurisdictions or still under investigation for potential use. Extracted from ZINC15 database, a total of 1394 FDA-approved, 2724 World-approved (not FDA-approved) and 1417 investigational molecules were used for drug repurposing.

Docking experiments

Hit compounds of the pharmacophore screening with a score value above a defined threshold were selected and

subjected to docking via AutoDock (Morris et al., 2009) and GOLD (Jones et al., 1997) docking tools. AutoDock tool uses a semi-empirical scoring function which combines molecular mechanics-based forcefield terms (e.g. vdW and electrostatics) and empirical terms such as solvation and ligand entropy. ChemPLP and GoldScore were the two in-house scoring functions selected for GOLD docking. In order to evaluate the accuracy of scoring functions, each of the seventeen agonists was redocked to its own receptor structure in the complex. The native state of each agonist was successfully predicted in all docking runs with satisfactorily low RMSD values below 2.0 Å.

The target protein used for the large database screening was the apo form of the crystal structure with PDB id 3bqd after removal of its agonist. It was arbitrarily chosen among seventeen receptors as they share a high degree of structural similarity (∼1-2 Å of RMSD). It should be noted that 3bqd is the deacylcortivazol bound form of the receptor and the expansion of the ligand binding site as a result of deacylcortivazol allowed docking of nonsteroidal ligands with various sizes that would not be fitted into an unbound form of the receptor and thus provided an ideal template for our screening studies in the search of both steroidal and nonsteroidal GR modulators (Suino-Powell et al., 2008).

The least successfully docked compounds were discarded based on a threshold value predefined for each scoring

Table 2. Features and screening results of six shared pharmacophore models along with ligand types and IDs.
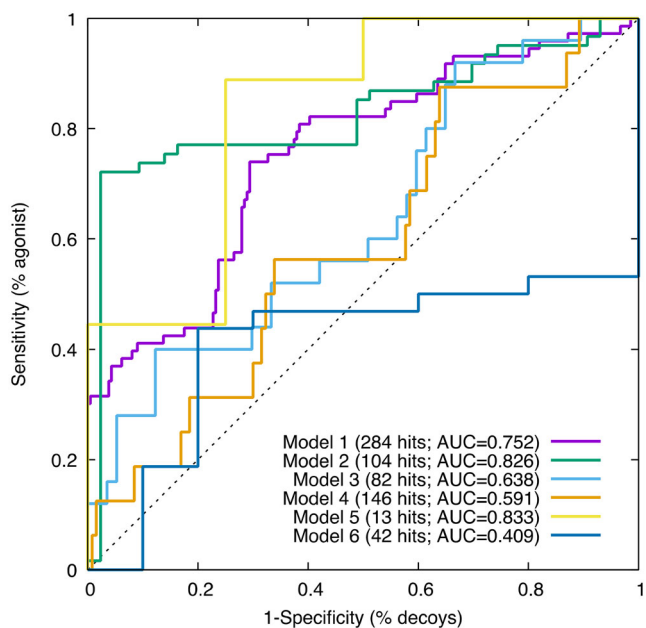
Shared Pharm. Model	Model ID	Ligand ids	H-bond Donor (HBD)	H-Bond Acceptor (HBA)	Hydrophobic (HPB)	# of hits (agonists/antagonists)	EF (5%/10%)
steroidal	1	DAY-CV7-DEX	1	1	2	284 (73/211)	5.0/4.8
	2	HCY-MOF-GW6	1	0	2	104 (61/43)	4.0/4.5
Non-steroidal	3	B9T-LSJ	1	0	2	82 (25/57)	3.7/3.1
	4	866-NN7	0	1	4	146 (16/130)	1.4/1.0
	5	JZN-JZS	2	1	3	13 (9/4)	5.0/5.0
	6	R8C-8W8-B9Q-B9W	1	1	4	42 (32/10)	2.5/3.7
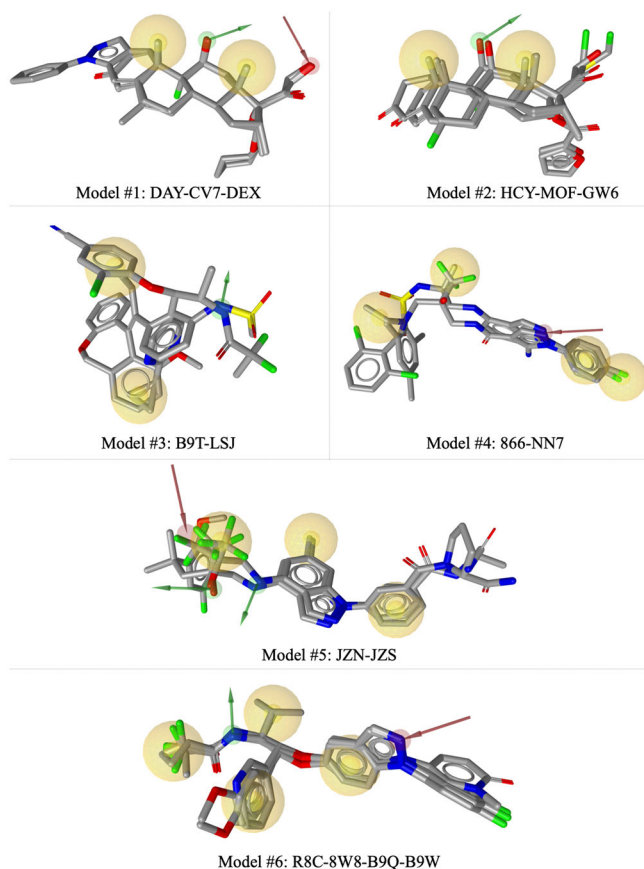
Figure 3. Representation of six shared pharmacophore models aligned to their corresponding agonist molecules.

Figure 4. Roc curves of the small database screening using six shared pharmacophore models. ($AUC_1 = 0.752$; $AUC_2 = 0.826$; $AUC_3 = 0.638$; $AUC_4 = 0.591$; $AUC_5 = 0.833$; $AUC_6 = 0.409$).

function. A total of 10 runs was executed for each docking experiment. The conformational search was established using a genetic algorithm in both AutoDock and GOLD. Dockings in AutoDock were confined in a rectangular box with dimensions of 18.75 Å x 18.75 Å x 18.75 Å and grid spacing of 0.375 Å, whereas in GOLD, a spherical region with 10 Å radius was created inside the binding pocket. Afterwards, all successfully docked compounds determined from three different scoring evaluations (AutoDock, ChemPLP and GoldScore) were merged to create a final set of compounds shared by all three hit lists.

Molecular dynamics (MD) simulations of hit compounds

Three hit compounds selected from the docking experiments and the steroid dexamethasone as a reference were each subjected to 100 ns long independent MD simulations in complex with the target receptor that was used for docking (PDB id: 3bqd). The drug-receptor complex was solvated in a box of TIP3P water molecules, and ionized with Na^{+2} and Cl^- to neutralize the total charge of the system. The whole system incorporated a total of 41,006 atoms of which 36,780 belonged to water molecules. OPLS-AA/M forcefield (Jorgensen et al., 1996) was employed for describing the interaction potential of both receptor and drug molecules. The forcefield parameters for drug molecules were generated via the Web-based service LigParGen (Jorgensen & Tirado-Rives, 2005). Using NAMD v2.13 software tool (Phillips et al., 2005), a 1000 steps of energy minimization was followed by 100 ns MD simulation for which the first 5 ns was taken as equilibration phase on the basis of the root mean square deviation (RMSD) profile. All simulations were conducted at constant NPT at 310 K using Langevin dynamics for all non-hydrogen atoms, with a Langevin damping coefficient of 5 ps^{-1}. The system was kept at a constant pressure of 1 atm by using a Node-Hoover Langevin piston (Feller et al., 1995) with a period of 100 fs and damping timescale of 50 ps. Long-range electrostatic interactions were treated by particle mesh Ewald (PME) method, with a grid point density of 1 A°. A cutoff of 12 A° was used for van der Waals and short-range electrostatics interactions with a switching function. Time step was set to 2 fs by using SHAKE algorithm for bonds involving hydrogens (Ryckaert et al., 1977) and the data was recorded at every 20 ps to generate a trajectory of 5000 conformations.
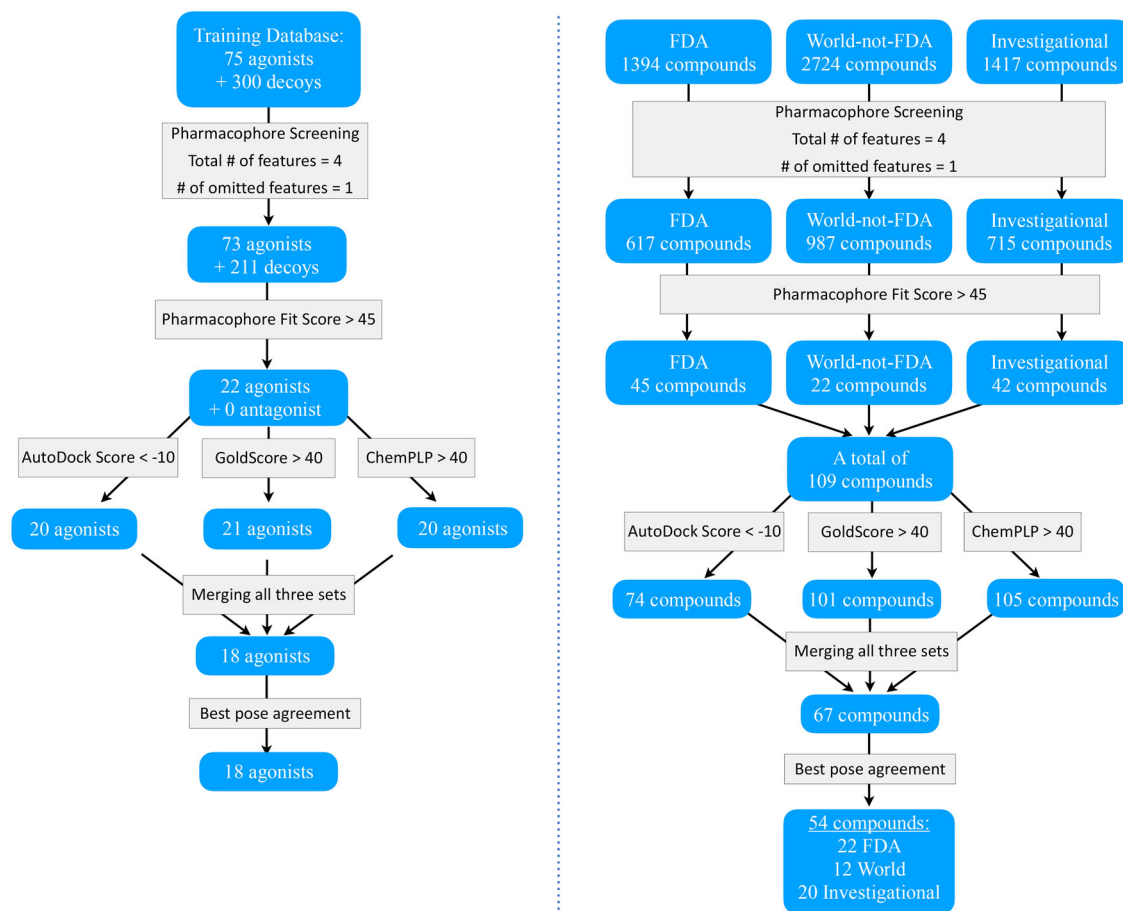
Figure 5. Flowchart for illustrating the screening protocol used to identify the hit compounds.

Results and discussion

Generation of "shared" pharmacophore models

As mentioned in Methods section, a pharmacophore model was created for each of seventeen complexes, two of which were illustrated in Figure 2 as the steroidal deacylcortivasol bound complex (PDB id: 3bqd) and the nonsteroidal indazole amide bound complex (PDB id: 3k23). The models of the remaining fifteen complexes were provided in Supplementary Figure 1. The hydrophobic features were represented with yellow spheres surrounding the atomic groups on the ligand, whereas hydrogen bond donor and acceptor groups were both represented with a sphere and an arrow. The red sphere corresponds to hydrogen bond acceptor group on the ligand and the red arrow emanating from the receptor simply points towards the acceptor group. Similarly, the green sphere represents the hydrogen bond donor group of the ligand and the green arrow emanates from the ligand towards its counterpart in the receptor. Table 1 gives the full list of the number of pharmacophore features for each complex along with ligand ids and PDB ids. Based on the similarity of their features, some of these models were grouped together to create a "shared" pharmacophore which incorporated the features shared by all its group members. The groups consisted of either two, three or four pharmacophore models as listed in Table 2 and also

depicted in Figure 3. This led to a total of seven distinct *shared* pharmacophore models which were further used for screening a small database in order to test each model's discriminatory power.

Critical assessment of "shared" pharmacophore models for discriminatory power

A small database composed of 75 agonists and 300 decoys (antagonists/unknown) was screened against each *shared* pharmacophore model to evaluate its capability to distinguish agonists from antagonists. Figure 4 illustrates ROC curves for each model along with its total number of hits and AUC values. Model #1 (DAY-CV71782-DEX) displayed the highest number of hits of 284 (73 agonists versus 211 decoys) with the highest enrichment factor of 5.0 and 4.8 in the top scoring 5% and top 10%, respectively (See last column in Table 2). Despite the fact that model #2 (HCY-MOF-GW6) had the highest AUC value of 0.826, none of the compounds in the hit list passed the Pharmacophore Fit score threshold of 45 which was selected as the "model exhaustion" point. On the other hand, 22 hits in model #1 had scores above 45 which yielded 100% true positives. For screening larger databases, the same threshold of 45 was used along with the selected pharmacophore model #1.
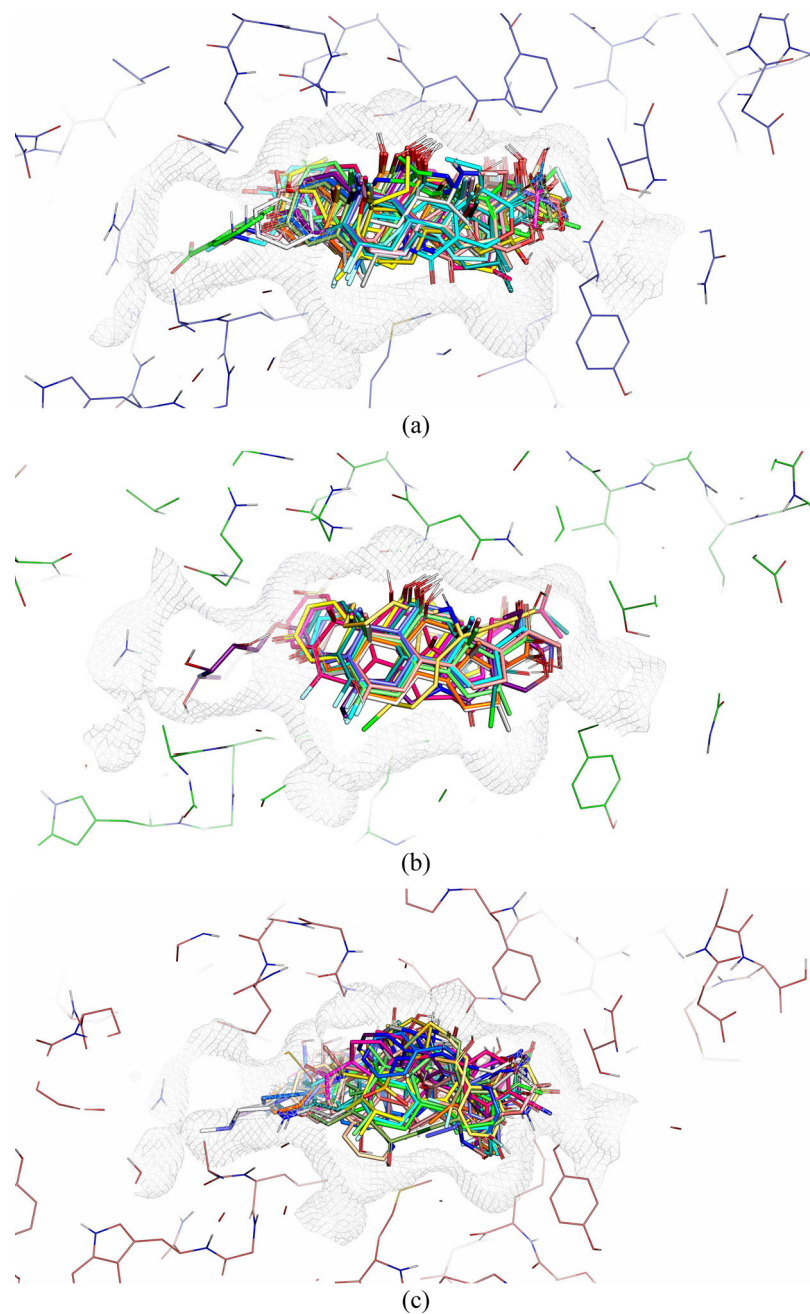
Figure 6. Best poses of the hit compounds in the binding pocket identified for a) FDA-approved, b) World-approved c) investigational databases.

Establishing thresholds for score values in docking-based virtual screening

Prior to screening the large database, 22 hit agonists having pharmacophore score value above 45 were subjected to docking. The goal here was to determine a threshold value for each score. For AutoDock, a threshold value of −10.0 kcal/mol was adopted such that the majority of the agonists in the list would be retained. As a result, only 2 out of 22 agonists were eliminated. Likewise, the threshold value was taken as 40 for both GoldScore and ChemPLP score values which led to a final list of 21 and 20 agonists respectively. As illustrated for the training database on the left side of the flowchart in Figure 5, all three docking results were later merged into a consensus list which consisted of compounds satisfying all three docking score thresholds. Accordingly, 18 agonists were left in the final hit list.

Final evaluation of the docked compounds in the binding pocket

In the final stage of filtering, three best poses obtained from three docking results, AutoDock, ChemPLP and GoldScore, were aligned to each other in the binding pocket in order to determine the consistency of the results. If either one of the best poses of one docking was different from another best pose by more than 4-5 Å, that compound was simply discarded from the hit list. Accordingly, none of 22 compounds showed inconsistency in their docked poses, thus were kept in the final hit list.
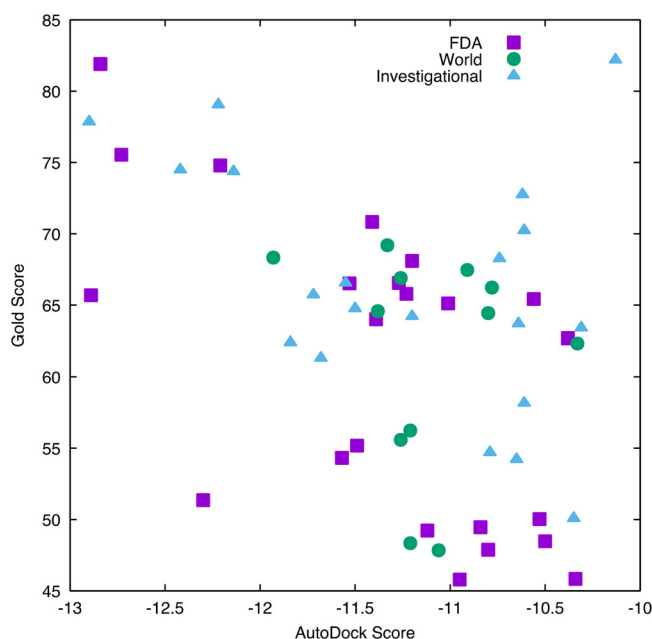
Figure 7. AutoDock score versus Gold score of 22 FDA-approved, 12 World-approved and 20 investigational hit compounds.

High-throughout virtual screening through pharmacophore screening and consensus docking of three databases

Three subsets of compounds extracted from ZINC database were subjected to pharmacophore screening using the selected pharmacophore model with ID #1. As indicated on the right side of the flowchart in Figure 5, nearly two thirds of the compounds in World-approved subsets were discarded at the first stage, simply because they didn't hold the required pharmacophore features. Also, both FDA-approved and investigational subsets diminished half in size at the end of the first stage of filtering. All the hit compounds satisfying the feature requirements were then evaluated based on their pharmacophore fit score value. A significant portion of compounds (> 90%) in each subset was discarded as they displayed a score value lower than 45. Once more, the highest elimination was observed for World-approved subset which lost nearly 98% of its content. As a result, 109 compounds in total from all three databases passed the second stage of filtering.

Each of 109 molecules was docked using different docking tools and scoring functions. The best pose extracted from each docking experiment was evaluated based on the corresponding predefined threshold value. Among three scoring evaluations, AutoDock yielded the least amount of compounds (75 out of 109) which satisfied the docking threshold, whereas the majority of compounds (>93%) passed the docking threshold for GoldScore and ChemPLP. Then, all the docked poses were merged to create a consensus pool which comprised a total of 67 hits satisfying all three docking threshold requirements. Among them, 27 were FDA-approved, 13 were World-approved and 27 were investigational compounds. Finally, any compound with its three best poses (one from each docking experiment) displaying a discordance in their relative orientation in the binding

pocket was simply discarded. Accordingly, 13 compounds were discarded and thus in the final hit list of 54 molecules, there were 22 FDA-approved, 12 World-approved and 20 investigational compounds of which their best pose was illustrated in Figure 6.

The corresponding ZINC database IDs, compound names (trade names if available) and all three score values were provided in two separate tables in Supplementary Tables 2 and 3 for each of 54 compounds. The order of the list in both tables was based on ChemPLP score from highest to lowest. Furthermore, AutoDock score was plotted against GoldScore value for each of 54 best poses as depicted in Figure 7 where a considerable amount of correlation between the two score values was observed especially for FDA-approved and investigational compounds. Same plot was created for ChemPLP versus AutoDock scores and a similar distribution profile was observed.

Additionally, all hit compounds were separately aligned to the pharmacophore model as illustrated in Figure 8a for steroids and Figure 8c for nonsteroids. It is clear that the hit compounds incorporated the most essential features of the model with satisfactory pharmacophore fit score values. Moreover, the neighbouring residues interacting with the hit compound was provided in Supplementary Table 1. Accordingly, five residues which interacted with more than 40 hit compounds were recognized as Asn564, Gly567, Met604, Phe623 and Gln642 (See grey shaded cells in the table). Among them, two polar uncharged residues, Asn564 and Gln642 interacted via hydrogen bonds with the majority of the compounds, whereas the hydrophobic residues Gly, Met and Phe were in close contact making short-range hydrophobic interactions. Furthermore, Asn564 and Gln642 were the two critical residues that interacted with all 17 ligands in the resolved complex structures which initially used to build the pharmacophore models. The interaction diagram of one selected steroidal and one nonsteroidal compound manifesting the highest score value in its category was also provided in Figure 8b and d. The 3 D version of the interacting residues nearby the compounds was also provided in Suppl Figure 2.

Critical assessment of three selected hit compounds via MD simulations

Two steroidal investigational (IDs:12a,13a) and one nonsteroidal FDA approved (ID:17c) compound were selected from the list of 54 hits. Their best poses with the receptor were used as the initial conformation for MD simulations. In addition, the well-known FDA approved steroid dexamethasone was used as a reference molecule for the critical assessment of our results. As illustrated in Figure 9a, in all four simulations, RMSD value of the protein with respect to its initial state ($t = 0\,ns$) indicated a stabilization of the structure within the first 5 ns. During 95 ns of production phase, there was no major structural deviation of the receptor from its initial state. RMSD profile of each drug compound in the complex was depicted in Figure 9b. Accordingly, dexamethasone and one steroidal compound (12a) preserved their initial
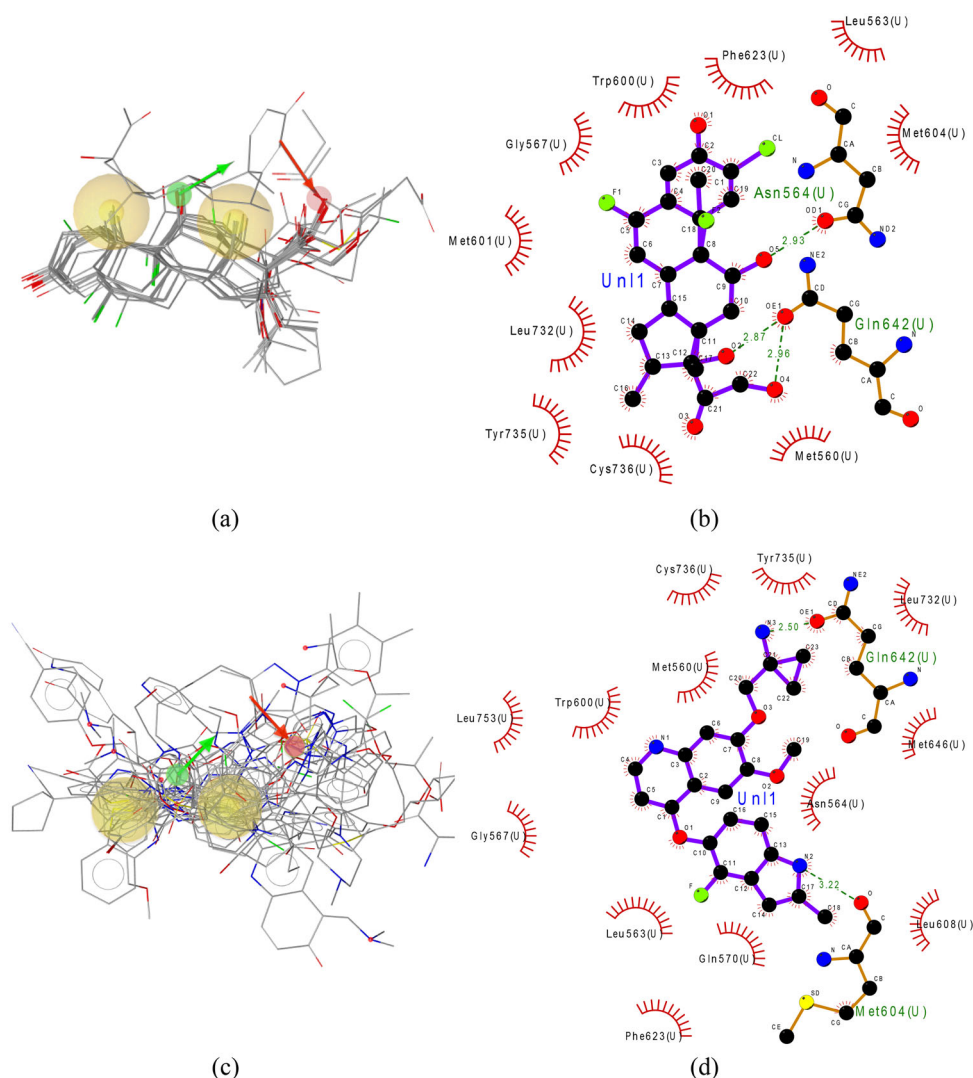
Figure 8. Hit compounds aligned to pharmacophore model along with an interaction diagram for one selected compound having the highest score value for (a, c) steroids and (b, d) nonsteroids.

conformations to a great extent, whereas compounds 13a and 17c rapidly changed their conformations by 2-3 Å in the early stages of the trajectory, yet preserved their states throughout the simulation.

Root mean square fluctuation profile of each system was illustrated in Figure 9c alongside the binding site residues indicated with red squares. No major difference was observed in the mobility of the receptor when bound to different compounds, except a few deviations observed in the loop regions. Binding site residues well coincided with the least mobile regions of the receptor which provided a stable interaction between the receptor and the drug molecule. The change in the radius of gyration of the complex was monitored throughout the trajectory as illustrated in Figure 9d. For all four complexes, the size of system was well preserved at its initial value, roughly 18.5 Å. Finally, the hydrogen bond network between the ligand and the receptor was investigated in detail for every snapshot in the trajectory. As illustrated in Figure 9e, the total number of hydrogen bonds between the drug compound and the receptor was monitored throughout the simulation. For the reference molecule dexamethasone, half of the snapshots

incorporated at least one hydrogen bond with the receptor. For the hit compounds 13a and 17c, one third of the trajectory displayed at least one hydrogen bond. On the other hand, the hit steroid compound 12a presented a total of five hydrogen bonds with the receptor in eight conformations, which was the highest number observed in all simulations. Nearly 70% of the time, compound 12a incorporated at least one hydrogen bond with the receptor, which indicated its strong binding affinity compared to the other compounds.

Moreover, neighbouring residues close to the bound ligand by less than 5 Å were determined and their frequency of occurrence over the entire trajectory was calculated. The list in Figure 9f shows a total of 24 residues with 100% occurrence in at least one of the drug-receptor simulations. 16 out of 24 residues highlighted in green were present in more than 97% of the collected 5000 snapshots. Finally, residues involved in hydrogen bonding with the ligand were indicated in red colour. *Met560*, *Leu563*, *Asn564*, *Gln570*, *Gln642*, *Cys736* were the most critical residues interacting via hydrogen bonds with the drug compound at all times in the majority of the four complexes.
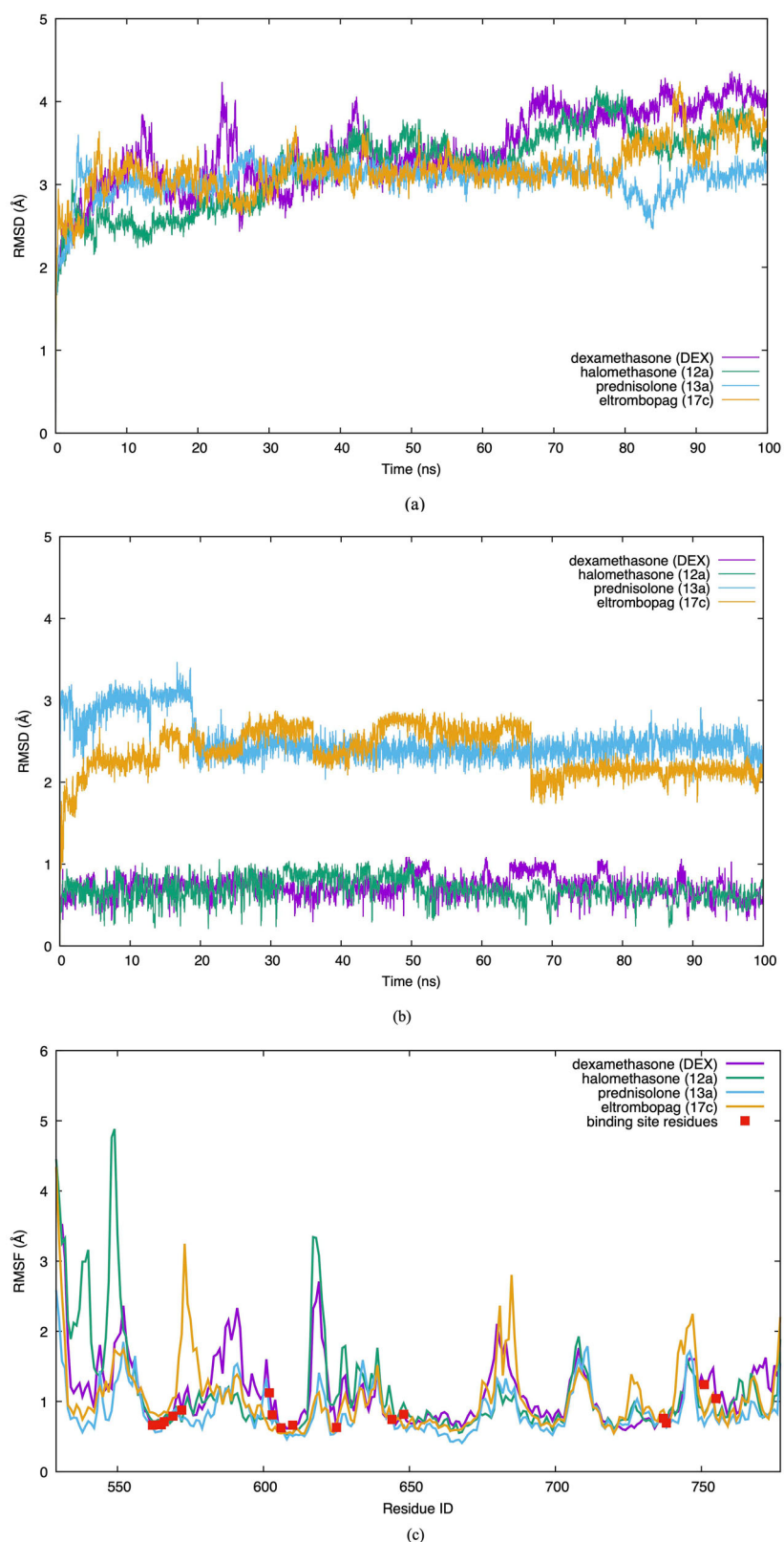
Figure 9. MD simulation analysis of four drug-receptor complexes. RMSD profiles of (a) the protein and (b) the drug compound with respect to the initial state. (c) RMSF profile with binding site residues. (d) Radius of gyration of the receptor (e) Hydrogen bond profile between drug and the receptor along with (f) the list of neighbouring residues (red coloured residues involved in hydrogen bond, residues in green cells had occurrences greater than 97%).

Further evaluation of possible agonist candidates for glucocorticoid receptor

Due to their common scaffolds, all of 35 steroidal hit compounds were further divided into two subcategories (models

A & B) using ChemMine tool. Table 3 lists 35 steroidal compounds categorized under models A and 10 steroidal compounds under model B. Two of those hits under model A, dexamethasone (ID:2a) and fluticasone furoate (ID:25a) were

(d)

(e)

	Met 560	Leu 563	Asn 564	Leu 566	Gly 567	Gln 570	Trp 600	Met 601	Met 604	Ala 605	Ala 607	Leu 608	Arg 611	Phe 623	Gln 642	Met 646	Lys 145	Leu 732	Tyr 735	Cys 736	Thr 739	Ile 747	Phe 749	Leu 753
DEX	100	100	100	100	100	100	100	100	100	100	31	100	49	100	100	100	-	100	100	100	100	96	97	97
12a	100	100	100	100	100	100	100	100	100	100	40	100	96	99	100	100	-	100	100	100	100	100	99	100
13a	100	100	100	100	100	100	100	100	100	99	97	100	90	100	99	99	0.5	100	100	100	100	73	100	100
17c	100	100	100	9	100	99	100	100	100	87	100	100	100	100	99	97	100	63	99	100	52	100	97	100

(f)

Figure 9. (Continued)

part of two of seventeen X-ray crystal complexes initially selected for constructing our screening protocol, and both appeared in our hit list with relatively high score values (See Supplementary Table 2). Moreover, GW870086 which is a potent anti-inflammatory compound identified by Uings et al. (Uings et al., 2013) shared the same steroid scaffold of model A with a unique set of side groups and listed in Table 3 for comparison. GW870086 was known with its distinctive ability to regulate only a subset of genes that are normally affected by classical GRs, thus presented itself as the most specific steroids available. Under model A, there were a total of six steroidal compounds from investigational subset (IDs: 11a, 12a, 13a, 14a, 15a and 16a), two of which were isomers (15a and 16a). Thus, our results highlighted

these compounds to be further investigated for potential GR modulators with fewer side effects.

Despite the fact that the shared pharmacophore model used for screening was derived from three steroidal compounds (dexamethasone (DEX), deacylcortivasol (DAY) and desisobuytyryl ciclesonide (CV71782)), 19 out of 54 hits were found to be nonsteroidal. Among 19, two pairs were found to be isomers, thus each of 17 compounds displayed unique structures as depicted in Table 4. In fact, it was not possible to cluster them based on their similarity due to their structural distinctiveness. Moreover, their structural similarities to experimentally reported nonsteroidal glucocorticoid modulators (Baiula & Spampinato, 2014; Bungard et al., 2011; López et al., 2008; Reuter et al., 2012; Ripa et al., 2018; Ripp et al.,
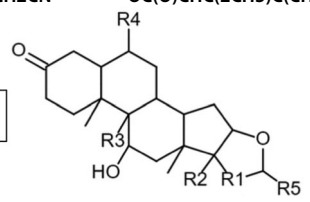
Table 3. A total of 35 steroidal hit compounds categorized under two groups based on the scaffolds represented as model A and B.

Model A

ID	R1	R2	R3'	R3''	R4	R5
1a		CH3	CH3	C(O)CH2CH3		
2a*		CH3	OH	C(O)CH2OH	F	
3a		CH3	OH	C(O)CH2OH	F	
4a	CH3		OH	C(O)CH3	F	
5a		OH	OH	C(O)CH2OH	F	
6a		CH3	OC(O)CH2CH3	C(O)CH2OC(O)CH2CH3	Cl	
7a	F	CH3	C(O)CH2OH		Cl	
8a			OH	C(O)CH2OH		
9a	CH3		OH	C(O)CH2OH		
10a			OH	C(O)CH2OH	F	
11a			OH	C(O)CH2OC(O)CH3		
12a	F	CH3	OH	C(O)CH2OH	F	Cl
13a			OH	C(O)CH2OC(O)2(CH2)C(OH)OH		
14a	CH3		OH	C(O)CH3	F	
15a			C(O)CH2OH	OC(O)3CH2CH3		
16a	CH3		OH	C(O)CH3	F	
17a	CH3		C(O)CH3			
18a	F		OH	C(O)CH2OH		
19a	F	CH3	OH	C(O)OH	F	
20a	F		C(O)CH2O	OC(O)2CH2CH3	F	
21a	F	CH3	OH	C(O)CH2O		
22a	F	CH3	C(O)CH2OH			
23a	F	CH3	C(O)CH2Cl	C(O)CH2CH3	F	
24a	F	CH3	OC(O)CH3	C(O)CH2OC(O)CH3	F	
25a**	F	CH3	OC(O)(C4H3O)	C(O)SCH2F	F	
GW***	**F**	**CH3**	**C(O)OCH2CN**	**OC(O)CHC(2CH3)C(CH3)**	**F**	

Model B

ID	R1	R2	R3	R4	R5
1b	N	C(O)CH2OC(O)CH3			CH3
2b	O	C(O)CH2OH		F	2CH3
3b	O	C(O)CH2OH			CH2CH2CH3
4b	O	C(O)CH2OH			2CH3
5b	O	C(O)CH2OH	F	F	2CH3
6b	O	C(O)CH2OC(O)CH3	F	F	2CH3
7b	O	C(O)CH2OC(O)CH3	F		C5H10
8b	O	C(O)CH2OH		F	2CH3
9b****	O	C(O)CH2OH		O	CH2CH2CH3
10b****	O	C(O)CH2OH		O	CH2CH2CH3

*Ligand in one of 17 X-ray structures used: PDB id 3cld.
**Ligand in one of 17 X-ray structures used: PDB id 4udc.
***GW870086: GR agonist acting as a potent anti-inflammatory agent.
****9 b and 10 b are isomers.
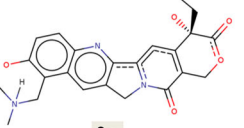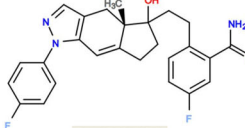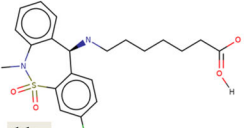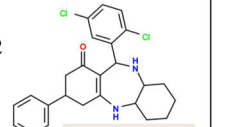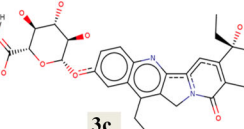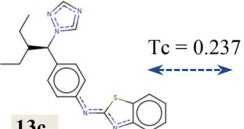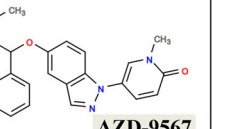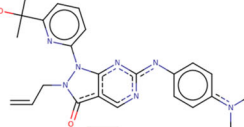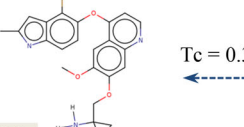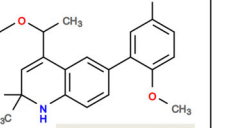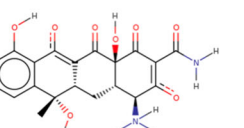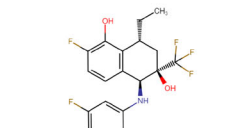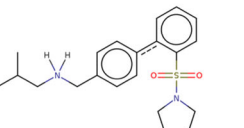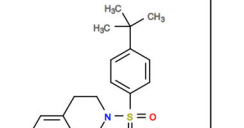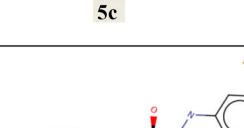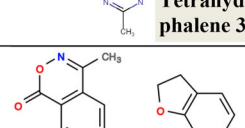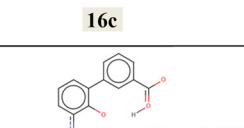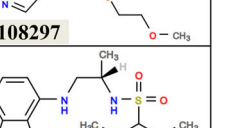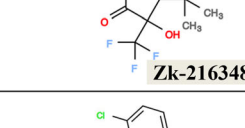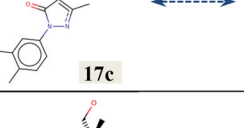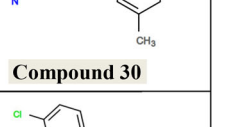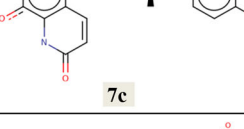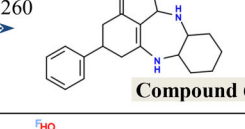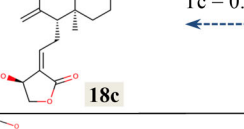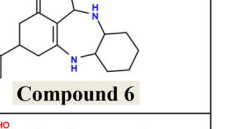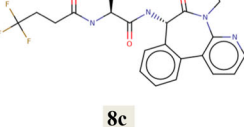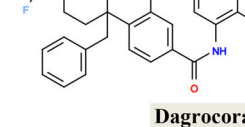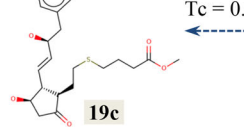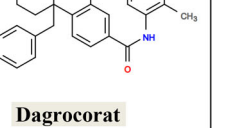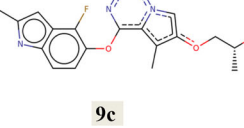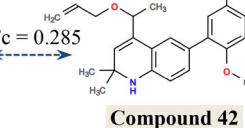
2018; van den Heuvel et al., 2016; van Lierop et al., 2012) were determined using Tanimoto coefficient (Tc) similarity index via ChemMine tool (Backman et al., 2011). For each nonsteroidal hit, the GR modulator with the highest similarity index was listed alongside in the table. Overall, the highest Tanimoto index was observed as 0.35 which was well below the accepted cutoff value of 0.5 for an acceptable degree of similarity.

Sorted by ChemPLP score values in Supplementary Table 2, the majority of compounds in the highest score range was nonsteroidal and belonged to investigational subset. As listed in Supplementary Table 3, anlotinib which is a nonsteroidal tyrosine kinase inhibitor displayed the highest ChemPLP (92.87) and the lowest negative AutoDock score values (-12.90) and it is still under investigation for lung and colorectal cancer treatment. Furthermore, as illustrated in Table 4, it shares the highest similarity (Tc = 0.339) with Compound-42 which was identified as a novel, potent and selective GR partial agonist by Takahashi et al. in 2007. In the high score range, there is another tyrosine kinase inhibitor which is brivanib alaninate and also shares the highest similarity (Tc = 0.285) with Compound-42. However, Tc values are well below 0.5 to

Table 4. A total of 17 nonsteroidal hit compounds and the experimentally identified GR modulator to which it shares the highest similarity indicated by Tanimoto coefficient (Tc).

2c — Tc = 0.265 — **MK-5932**	**11c** — Tc = 0.282 — **Compound 6**		
3c — Tc = 0.201 — **MK-5932**	**13c** — Tc = 0.237 — **AZD-9567**		
4c — Tc = 0.236 — **MK-5932**	**15c** — Tc = 0.339 — **Compound-42**		
5c — Tc = 0.200 — **Tetrahydraphalene 3**	**16c** — Tc = 0.225 — **C108297**		
6c — Tc = 0.227 — **Zk-216348**	**17c** — Tc = 0.350 — **Compound 30**		
7c — Tc = 0.260 — **Compound 6**	**18c** — Tc = 0.134 — **Compound 6**		
8c — Tc = 0.270 — **Dagrocorat**	**19c** — Tc = 0.162 — **Dagrocorat**		
9c — Tc = 0.285 — **Compound 42**	**20c** — Tc = 0.305 — **Dagrocorat**		
10c — Tc = 0.185 — **Tetrahydraphalene 3**			

suggest any striking structural similarity. Unlike steroidal compounds which were either GR agonist or metabolite, nonsteroidal compounds in the hit list displayed different activities such as G-protein coupled receptor (GPCR) agonists, retinoic acid metabolism inhibitor, topoisomerase inhibitor, androgen receptor modulator, and an antibiotic tetracycline. The fact that none of the nonsteroidal compounds were GR agonists propose them as alternative candidates of which the majority was still under investigational stages (14 investigational versus 3 FDA-approved and 2 World-approved). Thus, each of these compounds used for the treatment of various diseases can be repurposed as GR modulators.

Conclusions

Thousands of compounds from FDA-approved, World-approved and investigational databases were screened using a *shared* pharmacophore model holding the common pharmacophore features of three known crystal structures of GR receptor in complex with their steroidal agonists. Nearly half of the compounds in each database satisfied the shared pharmacophore features, yet a significant portion of them ($>$90%) was discarded after filtering with a threshold score value of 45. This threshold value was determined after a small database composed of 75 agonists and 300 decoys (antagonists/unknown) was screened. None of the antagonists with the *shared* pharmacophore features displayed a score value greater than 45, thus discarded, whereas the majority ($\sim$30%, 22 out of 75) of screened agonists had scores well above that threshold.

Out of 5535 compounds, a total of 110 satisfying all the pharmacophore requirements were subjected to three different docking experiments for further evaluation as potential binders. Similar to pharmacophore screening, different thresholds were determined for each docking evaluation using the small database, prior to screening the large database. As a result, the majority of the compounds satisfied the predefined thresholds, especially in Goldscore and ChemPLP scoring evaluations. Upon merging the results by extracting the compounds that displayed desired affinities towards GR in all three docking experiments, a pool of 67 compounds was obtained. Finally, three best poses of each compound collected from three docking were aligned and compared to each other, and the compounds which displayed different conformations/orientations in their best pose were simply discarded. In the final evaluation step, 100 ns long MD simulations were conducted on complex systems with three selected compounds from the hit list along with the known agonist dexamethasone used as a reference. Throughout the simulations, all three drug compounds formed stable interactions with the receptor via multiple hydrogen bonds with several residues commonly observed in dexamethasone-GR complex.

In the final hit list of 54 compounds, 35 were steroidal GR agonists. The remaining 19 compounds were nonsteroidal despite the fact that the initial *shared* pharmacophore model was constructed from receptor structures in complex with steroidal compounds. Each of 19 compounds displayed unique structures with a low degree of similarity to experimentally reported nonsteroidal GR modulators. Consequently, even though the experimental validation lacks, the distinctiveness of each of these compounds might pave the way for their repurposing to achieve potential agonist activities with fewer side effects, when used in appropriate dosages.

ORCID

Ebru Demet Akten (iD) http://orcid.org/0000-0002-0358-3171

Availability of data and material

Available if required.

Code availability

Available if required.

Author contributions

The manuscript was written through the contributions of all authors. All authors have given approval to the final version of the manuscript.

References

Ashburn, T. T., & Thor, K. B. (2004). Drug repositioning: Identifying and developing new uses for existing drugs. *Nature Reviews. Drug Discovery*, *3*(8), 673–683. https://doi.org/10.1038/nrd1468

Backman, T. W. H., Cao, Y., & Girke, T. (2011). ChemMine tools: An online service for analyzing and clustering small molecules. *Nucleic Acids Research*, *39*(Web Server issue), W486–W491. https://doi.org/10.1093/nar/gkr320

Baiula, M., & Spampinato, S. (2014). Mapracorat, a Novel non-steroidal selective glucocorticoid receptor agonist for the treatment of allergic conjunctivitis. *Inflammation & Allergy Drug Targets*, *13*(5), 289–298. https://doi.org/10.2174/1871528113666141106101356

Bereshchenko, O., Bruscoli, S., & Riccardi, C. (2018). Glucocorticoids, sex hormones, and immunity. *Frontiers in Immunology*, *9*, 1332–1310. https://doi.org/10.3389/fimmu.2018.01332

Berger, M., Rehwinkel, H., Schmees, N., Schäcke, H., Edman, K., Wissler, L., Reichel, A., & Jaroch, S. (2017). Discovery of new selective glucocorticoid receptor agonist leads. *Bioorganic & Medicinal Chemistry Letters*, *27*(3), 437–442. https://doi.org/10.1016/j.bmcl.2016.12.047

Biggadike, K., Bledsoe, R. K., Coe, D. M., Cooper, T. W. J., House, D., Iannone, M. A., Macdonald, S. J. F., Madauss, K. P., McLay, I. M., Shipley, T. J., Taylor, S. J., Tran, T. B., Uings, I. J., Weller, V., & Williams, S. P. (2009). Design and X-ray crystal structures of high-potency nonsteroidal glucocorticoid agonists exploiting a novel binding site on the receptor. *Proceedings of the National Academy of Sciences of the United States of America*, *106*(43), 18114–18119. https://doi.org/10.1073/pnas.0909125106

Biggadike, K., Bledsoe, R. K., Hassell, A. M., Kirk, B. E., McLay, I. M., Shewchuk, L. M., & Stewart, E. L. (2008). X-ray crystal structure of the novel enhanced-affinity glucocorticoid agonist fluticasone furoate in the glucocorticoid receptor-ligand binding domain. *Journal of Medicinal Chemistry*, *51*(12), 3349–3352. https://doi.org/10.1021/jm800279t

Bledsoe, R. K., Montana, V. G., Stanley, T. B., Delves, C. J., Apolito, C. J., McKee, D. D., Consler, T. G., Parks, D. J., Stewart, E. L., Willson, T. M., Lambert, M. H., Moore, J. T., Pearce, K. H., & Xu, H. E. (2002). Crystal structure of the glucocorticoid receptor ligand binding domain reveals a novel mode of receptor dimerization and coactivator recognition. *Cell*, *110*(1), 93–105. https://doi.org/10.1016/S0092-8674(02)00817-6

Bungard, C. J., Hartman, G. D., Manikowski, J. J., Perkins, J. J., Bai, C., Brandish, P. E., Euler, D. H., Hershey, J. C., Schmidt, A., Fang, Y., Norcross, R. T., Rushmore, T. H., Thompson, C. D., & Meissner, R. S. (2011). Discovery of selective glucocorticoid receptor modulator MK-5932. *Bioorganic & Medicinal Chemistry*, *19*(24), 7374–7386. https://doi.org/10.1016/j.bmc.2011.10.054

Carson, M. W., Luz, J. G., Suen, C., Montrose, C., Zink, R., Ruan, X., Cheng, C., Cole, H., Adrian, M. D., Kohlman, D. T., Mabry, T., Snyder, N., Condon, B., Maletic, M., Clawson, D., Pustilnik, A., & Coghlan, M. J. (2014). Glucocorticoid receptor modulators informed by crystallography lead to a new rationale for receptor selectivity, function, and implications for structure-based design. *Journal of Medicinal Chemistry*, *57*(3), 849–860. https://doi.org/10.1021/jm401616g

Coghlan, M. J., Kym, P. R., Elmore, S. W., Wang, A. X., Luly, J. R., Wilcox, D., Stashko, M., Lin, C. W., Miner, J., Tyree, C., Nakane, M., Jacobson, P., & Lane, B. C. (2001). Synthesis and characterization of non-steroidal ligands for the glucocorticoid receptor: selective quinoline derivatives with prednisolone-equivalent functional activity. *Journal of Medicinal Chemistry*, *44*(18), 2879–2885. https://doi.org/10.1021/jm010228c

De Bosscher, K., Vanden Berghe, W., Beck, I. M. E., Van Molle, W., Hennuyer, N., Hapgood, J., Libert, C., Staels, B., Louw, A., & Haegeman, G. (2005). A fully dissociated compound of plant origin for inflammatory gene repression. *Proceedings of the National Academy of Sciences of the United States of America*, *102*(44), 15827–15832. https://doi.org/10.1073/pnas.0505554102

Edman, K., Ahlgren, R., Bengtsson, M., Bladh, H., Bäckström, S., Dahmén, J., Henriksson, K., Hillertz, P., Hulikal, V., Jerre, A., Kinchin, L., Kåse, C., Lepistö, M., Mile, I., Nilsson, S., Smailagic, A., Taylor, J., Tjörnebo, A., Wissler, L., & Hansson, T. (2014). The discovery of potent and selective non-steroidal glucocorticoid receptor modulators, suitable for inhalation. *Bioorganic & Medicinal Chemistry Letters*, *24*(11), 2571–-2577. https://doi.org/10.1016/j.bmcl.2014.03.070

Edman, K., Hosseini, A., Bjursell, M. K., Bjursell, M. K., Aagard, A., Wissler, L., Gunnarsson, A., Kaminski, T., Köhler, C., Bakström, S., Jensen, T. J., Cavallin, A., Karlsson, U., Nilsson, E., Lecina, D., Takahashi, R., Grebner, C., Geschwindner, S., Lepisto, M., Hogner, A. C., & Guallar, V. (2015). Ligand binding mechanism in steroid receptors: From conserved plasticity to differential evolutionary constraints. *Structure (London, England: 1993)*, *23*(12), 2280–2290. https://doi.org/10.1016/j.str.2015.09.012

Feller, S. E., Zhang, Y. H., & Pastor, R. W. (1995). Computer-simulation of liquid/liquid interfaces 2. Surface-tension area dependence of a bilayer and monolayer. *Journal of Chemical Physics*, *103*(23), 10267–10276. https://doi.org/10.1063/1.469928

He, Y., Yi, W., Suino-Powell, K., Zhou, X. E., Tolbert, W. D., Tang, X., Yang, J., Yang, H., Shi, J., Hou, L., Jiang, H., Melcher, K., & Xu, H. E. (2014). Structures and mechanism for the design of highly potent glucocorticoids. *Cell Research*, *24*(6), 713–726. https://doi.org/10.1038/cr.2014.52

Hemmerling, M., Nilsson, S., Edman, K., Eirefelt, S., Russell, W., Hendrickx, R., Johnsson, E., Kärrman Mårdh, C., Berger, M., Rehwinkel, H., Abrahamsson, A., Dahmén, J., Eriksson, A. R., Gabos, B., Henriksson, K., Hossain, N., Ivanova, S., Jansson, A.-H., Jensen, T. J., … Hansson, T. (2017). Selective nonsteroidal glucocorticoid receptor modulators for the inhaled treatment of pulmonary diseases. *Journal of Medicinal Chemistry*, *60*(20), 8591–8605. https://doi.org/10.1021/acs.jmedchem.7b01215

Humphrey, W., Dalke, A., & Schulten, K. (1996). VMD: visual molecular dynamics. *Journal of Molecular Graphics*, *14*(1), 33–38. https://doi.org/10.1016/0263-7855(96)00018-5

Jaroch, S., Berger, M., Huwe, C., Krolikiewicz, K., Rehwinkel, H., Schäcke, H., Schmees, N., & Skuballa, W. (2010). Discovery of quinolines as selective glucocorticoid receptor agonists. *Bioorganic & Medicinal*

Chemistry Letters, *20*(19), 5835–5838. https://doi.org/10.1016/j.bmcl.2010.07.125

Jones, G., Willett, P., Glen, R. C., Leach, A. R., & Taylor, R. (1997). Development and validation of a genetic algorithm for flexible docking. *Journal of Molecular Biology*, *267*(3), 727–748. https://doi.org/10.1006/jmbi.1996.0897

Jorgensen, W. L., & Tirado-Rives, J. (2005). Potential energy functions for atomic-level simulations of water and organic and biomolecular systems. *Proceedings of the National Academy of Sciences of the United States of America*, *102*(19), 6665–6670. https://doi.org/10.1073/pnas.0408037102

Jorgensen, W. L., Maxwell, D. S., & Tirado-Rives, J. (1996). Development and testing of the OPLS all-atom force field on conformational energetics and properties of organic liquids. *Journal of the American Chemical Society*, *118*(45), 11225–11236. https://doi.org/10.1021/ja9621760

Kadmiel, M., & Cidlowski, J. A. (2013). Glucocorticoid receptor signaling in health and disease. *Trends in Pharmacological Sciences*, *34*(9), 518–530. https://doi.org/10.1016/j.tips.2013.07.003

Karra, A. G., Konstantinou, M., Tzortziou, M., Tsialtas, I., Kalousi, F. D., Garagounis, C., Hayes, J. M., & Psarra, A. M. G. (2019). Potential dissociative glucocorticoid receptor activity for protopanaxadiol and protopanaxatriol. *International Journal of Molecular Sciences*, *20*, 94. https://doi.org/10.3390/ijms20010094

Kim, S., Chen, J., Cheng, T., Gindulyte, A., He, J., He, S., Li, Q., Shoemaker, B. A., Thiessen, P. A., Yu, B., Zaslavsky, L., Zhang, J., & Bolton, E. E. (2019). PubChem 2019 update: Improved access to chemical data. *Nucleic Acids Research*, *47*(D1), D1102–D1109. https://doi.org/10.1093/nar/gky1033

López, F. J., Ardecky, R. J., Bebo, B., Benbatoul, K., De Grandpre, L., Liu, S., Leibowitz, M. D., Marschke, K., Rosen, J., Rungta, D., Viveros, H. O., Yen, W.-C., Zhi, L., Negro-Vilar, A., & Miner, J. N. (2008). LGD-5552, an antiinflammatory glucocorticoid receptor ligand with reduced side effects, in vivo. *Endocrinology*, *149*(5), 2080–2089. https://doi.org/10.1210/en.2007-1353

Madauss, K. P., Bledsoe, R. K., Mclay, I., Stewart, E. L., Uings, I. J., Weingarten, G., & Williams, S. P. (2008). The first X-ray crystal structure of the glucocorticoid receptor bound to a non-steroidal agonist. *Bioorganic & Medicinal Chemistry Letters*, *18*(23), 6097–6099. https://doi.org/10.1016/j.bmcl.2008.10.021

Morris, G. M., Huey, R., Lindstrom, W., Sanner, M. F., Belew, R. K., Goodsell, D. S., & Olson, A. J. (2009). Autodock4 and AutoDockTools4: Automated docking with selective receptor flexibility. *Journal of Computational Chemistry*, *30*(16), 2785–2791. https://doi.org/10.1002/jcc.21256

Mysinger, M. M., Carchia, M., Irwin, J. J., & Shoichet, B. K. (2012). Directory of Useful Decoys, Enhanced (DUD-E): Better ligands and decoys for better benchmarking. *Journal of Medicinal Chemistry*, *55*(14), 6582–6594. https://doi.org/10.1021/jm300687e

Oakley, R. H., & Cidlowski, J. A. (2011). Cellular processing of the glucocorticoid receptor gene and protein: New mechanisms for generating tissue-specific actions of glucocorticoids. *The Journal of Biological Chemistry*, *286*(5), 3177–3184. https://doi.org/10.1074/jbc.R110.179325

Onnis, V., Kinsella, G. K., Carta, G., Jagoe, W. N., Price, T., Williams, D. C., Fayne, D., & Lloyd, D. G. (2010). Virtual screening for the identification of novel nonsteroidal glucocorticoid modulators. *Journal of Medicinal Chemistry*, *53*(8), 3065–3074. https://doi.org/10.1021/jm901452y

Phillips, J. C., Braun, R., Wang, W., Gumbart, J., Tajkhorshid, E., Villa, E., Chipot, C., Skeel, R. D., Kale, L., & Schulten, K. (2005). Scalable molecular dynamics with NAMD. *Journal of Computational Chemistry*, *26*(16), 1781–1802. https://doi.org/10.1002/jcc.20289

Potamitis, C., Siakouli, D., Papavasileiou, K. D., Boulaka, A., Ganou, T. V., Roussaki, M., Calogeropoulou, T., Zoumpoulakis, P., Alexis, M. N., Zervou, M., & Mitsiou, D. J. (2019). Discovery of New non-steroidal selective glucocorticoid receptor agonists. *The Journal of Steroid Biochemistry and Molecular Biology*, *186*, 142–153. https://doi.org/10.1016/j.jsbmb.2018.10.007

Reuter, K., Loitsch, S. M., Dignass, A. U., Steinhilber, D., & Stein, J. (2012). Selective nonsteroidal glucocorticoid receptor agonists attenuate inflammation but do not impair intestinal epithelial cell restitution in

vitro. *PLoS One*, *7*(1), 1–14. https://doi.org/10.1371/journal.pone.0029756

Ripa, L., Edman, K., Dearman, M., Edenro, G., Hendrickx, R., Ullah, V., Chang, H. F., Lepistö, M., Chapman, D., Geschwindner, S., Wissler, L., Svanberg, P., Lawitz, K., Malmberg, J., Nikitidis, A., Olsson, R. I., Bird, J., Llinas, Hegelund-Myrback, T., … Drmota, T. (2018). A discovery of a novel oral glucocorticoid receptor modulator (AZD9567) with improved side effect profile. *Journal of Medicinal Chemistry*, *61*(5), 1785–1799. https://doi.org/10.1021/acs.jmedchem.7b01690

Ripp, S. L., Mukherjee, A., Eng, H., Stock, T., Fleishaker, D., Checchio, T., & Tammara, B. (2018). In vitro and in vivo investigation of potential for complex CYP3A interaction for PF-00251802 (Dagrocorat), a novel dissociated agonist of the glucocorticoid receptor. *Clinical Pharmacology in Drug Development*, *7*(3), 244–255. https://doi.org/10.1002/cpdd.411

Ryckaert, J. P., Ciccotti, G., & Berendsen, H. J. C. (1977). Numerical-integration of cartesian equations of motion of a system with constraints - molecular-dynamics of N-alkanes. *Journal of Computational Physics*, *23*(3), 327–341. https://doi.org/10.1016/0021-9991(77)90098-5

Schäcke, H., Schottelius, A., Döcke, W.-D., Strehlke, P., Jaroch, S., Schmees, N., Rehwinkel, H., Hennekes, H., & Asadullah, K. (2004). Dissociation of transactivation from transrepression by a selective glucocorticoid receptor agonist leads to separation of therapeutic effects from side effects. *Proceedings of the National Academy of Sciences of the United States of America*, *101*(1), 227–232. https://doi.org/10.1073/pnas.0300372101

Schäcke, H., Zollner, T. M., Döcke, W. D., Rehwinkel, H., Jaroch, S., Skuballa, W., Neuhaus, R., May, E., Zügel, U., & Asadullah, K. (2009). Characterization of ZK 245186, a novel, selective glucocorticoid receptor agonist for the topical treatment of inflammatory skin diseases. *British Journal of Pharmacology*, *158*(4), 1088–1103. https://doi.org/10.1111/j.1476-5381.2009.00238.x

Schake, H., Döcke, W. D., & Asadullah, K. (2002). Mechanisms involved in the side effects of glucocorticoids. *Pharmacology & Therapeutics*, *96*, 23–43.

Sterling, T., & Irwin, J. J. (2015). ZINC 15-ligand discovery for everyone. *Journal of Chemical Information and Modeling*, *55*(11), 2324–2337. https://doi.org/10.1021/acs.jcim.5b00559

Suino-Powell, K., Xu, Y., Zhang, C., Tao, Y. G., Tolbert, D. T., Simons, S. S., & Xu, H. E. (2008). Doubling the size of the glucocorticoid receptor ligand binding pocket by deacylcortivazol. *Molecular and Cellular Biology*, *28*(6), 1915–1923. https://doi.org/10.1128/MCB.01541-07

Uings, I. J., Needham, D., Matthews, J., Haase, M., Austin, R., Angell, D., Leavens, K., Holt, J., Biggadike, K., & Farrow, S. N. (2013). Discovery of GW870086: A potent anti-inflammatory steroid with a unique pharmacological profile. *British Journal of Pharmacology*, *169*(6), 1389–1403. https://doi.org/10.1111/bph.12232

van den Heuvel, J. K., Boon, M. R., van Hengel, I., van der Put, E. P., van Beek, L., van Harmelen, V., van Dijk, K. W., Pereira, A. M., Hunt, H., Belanoff, J. K., Rensen, P. C. N., & Meijer, O. C. (2016). Identification of a selective glucocorticoid receptor modulator that prevents both diet-induced obesity and inflammation . *British Journal of Pharmacology*, *173*(11), 1793–1804. https://doi.org/10.1111/bph.13477

van Lierop, M. J. C., Alkema, W., Laskewitz, A. J., Dijkema, R., van der Maaden, H. M., Smit, M. J., Plate, R., Conti, P. G. M., Jans, C. G. J. M., Timmers, C. M., van Boeckel, C. A. A., Lusher, S. J., McGuire, R., van Schaik, R. C., de Vlieg, J., Smeets, R. L., Hofstra, C. L., Boots, A. M. H., van Duin, M., Ingelse, B. A., Schoonen, W. G. E. J., … Dokter, W. H. A. (2012). Org 214007-0: A novel nonsteroidal selective glucocorticoid receptor modulator with full anti-inflammatory properties and improved therapeutic index. *PLOS One*, *7*, 1–15. https://doi.org/10.1371/journal.pone.0048385

Wolber, G., & Langer, T. (2005). LigandScout: 3-D pharmacophores derived from protein-bound ligands and their use as virtual screening filters. *Journal of Chemical Information and Modeling*, *45*(1), 160–169. https://doi.org/10.1021/ci049885e